Stable Atom-Scale Junctions on Silicon Fabricated by Kinetically Controlled Electrochemical Deposition and Dissolution

Ping Shi and Paul W. Bohn*

Department of Chemical and Biomolecular Engineering, University of Notre Dame, Notre Dame, Indiana 46556

ABSTRACT Metallic atom-scale junctions (ASJs) constitute the natural limit of nanowires, in which the limiting region of conduction is only a few atoms wide. They are of interest because they exhibit ballistic conduction and their conductance is extraordinarily sensitive to molecular adsorption. However, identifying robust and regenerable mechanisms for their production is a challenge. Gold ASJs have been fabricated electrochemically on silicon using an iodide-containing medium to control the kinetics. Extremely slow electrodeposition or electrodissolution rates were achieved and used to reliably produce ASJs with limiting conductance $<5\ G_0$. Starting from a photolithographically fabricated, Si_3N_4-protected micrometer-scale Au bridge between two contact electrodes, a nanometer-scale gap was prepared by focused ion beam milling. The opposing Au faces of this construct were then used in an open-circuit working electrode configuration to produce Au ASJs, either directly or by first overgrowing a thicker Au nanowire and electrothinning it back to an ASJ. Gold ASJs produced by either approach exhibit good stability—in some cases being stable over hours at 300 K—and quantized conductance properties. The influence of deposition/dissolution potential and supporting electrolyte on the stability of ASJs are considered.

KEYWORDS: electrodeposition · nanofabrication · atom-scale junction · metal nanowire · electrodissolution

Metal nanowires and nanocontacts have received a great deal of attention recently both in nanoelectronics[1,2] and in chemical sensing[3–10] due to their unique properties. For example, the conductance of metal nanowires decreases upon molecular adsorption due to scattering of conduction electrons by adsorbate−image charge interactions,[7–9,11–16] with thinner wires exhibiting larger effects. In this regard, atomically thin metal wires (or atom-scale junctions, ASJs) hold great promise for highly sensitive nanostructured chemical sensors for several reasons. First, the total number of molecules that can be accommodated on an ASJ surface is limited by the exposed surface area and can be quite small (*e.g.*, of the order of 10^3-10^4 molecules). Since measurements of very small changes in absolute surface population (±5 molecules) have been demonstrated,[15] it is clearly possible to achieve high sensitivity detection using ASJs. Second, the small junctions are compatible with micro- and nanoelectronic architectures, and the detection method is purely electrical, indicating that ASJs can be engineered into economical, portable devices for chemical detection.

When the size of a conductor is of the order of its Fermi wavelength, λ_F, unique quantum conduction phenomena may arise. For example, the conductance is quantized by

$$G = (2e^2/h)\sum_{i=1}^{n} T_i \qquad (1)$$

where e is the electron charge, h is Planck's constant, and T_i is the transmission probability of the ith conduction channel (quantum mode).[17–20] For ideal metals, such as gold, $T_i = 1$ for all channels. Hence the conductance is quantized in the form of $G = nG_0$, where $G_0 = 2e^2/h = 1/(12.9\ \text{k}\Omega)$ is the conductance quantum, and the number of quantum modes, n, is dependent on the size of the conductor. For typical metals, $\lambda_F < 1$ nm, which is the characteristic size of an atom-scale junction. Therefore, one can simply monitor the quantization of conductance electrically to determine the formation of an ASJ, a task that is difficult by conventional microscopy since the ASJs are extremely small and may be buried beneath intervening material layers.

To date, several methods have been developed to fabricate ASJs, including mechanically controllable break junctions (MCBJs)[21] and techniques based on scanning tunneling microscopy (STM).[19,22] In addition, electrochemical methods[23–29] are

*Address correspondence to pbohn@nd.edu.

Received for review May 17, 2008 and accepted July 10, 2008.

Published online July 25, 2008.
10.1021/nn8002955 CCC: $40.75

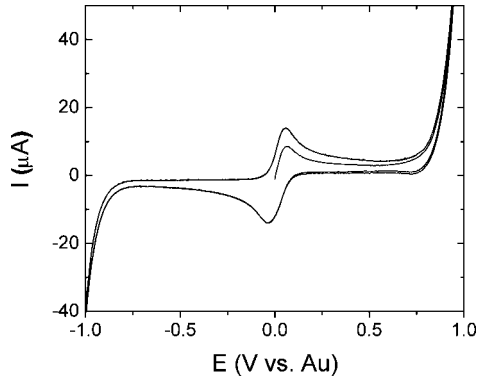

Figure 1. Cyclic voltammogram of a macroscopic Au wire (0.25 mm diameter) in the iodide-containing electroplating medium (see text for details). CE and QRE: Au wire (same diameter); potential scan rate = 100 mV/s.

attractive, especially for ultimate deployment in unattended chemical sensors. Electrochemical methods do not require expensive instrumentation and are completely free of mechanical deformation, which is undesirable in chip-based nanodevices. Electrochemistry can produce planar stand-alone nanojunctions that are less vulnerable to environmental perturbations and thus exhibit good stability. Electrochemical reaction, chosen properly, are reversible, and either electrodeposition or electrodissolution can be used to fabricate—or repair—the junctions.

Nevertheless, fabrication of ASJs with long-term (>100 s) stability remains challenging. Thus, to utilize these unique nanostructures for sensing applications, a routine electrochemical fabrication protocol capable of producing robust and regenerable ASJs on Si at room temperature would be highly desirable. One of the principal difficulties is achieving sufficient control over the rate of ASJ formation. Ideally, the deposition or dissolution should proceed at an extremely slow rate when the metal nanogap or nanowire approaches atomic dimensions. Moreover, the lifetime and stability of ASJs should be long and strong enough to introduce analytes and record the conductance change induced by adsorbates. Here, we report a new mode of electrochemical nanofabrication, producing extremely slow electrochemical deposition/dissolution rates, thereby enhancing the controllability of ASJ fabrication. In addition, by carefully selecting the electroplating media, the gold atom-scale junctions may be prepared that are stable from tens of minutes to hours.

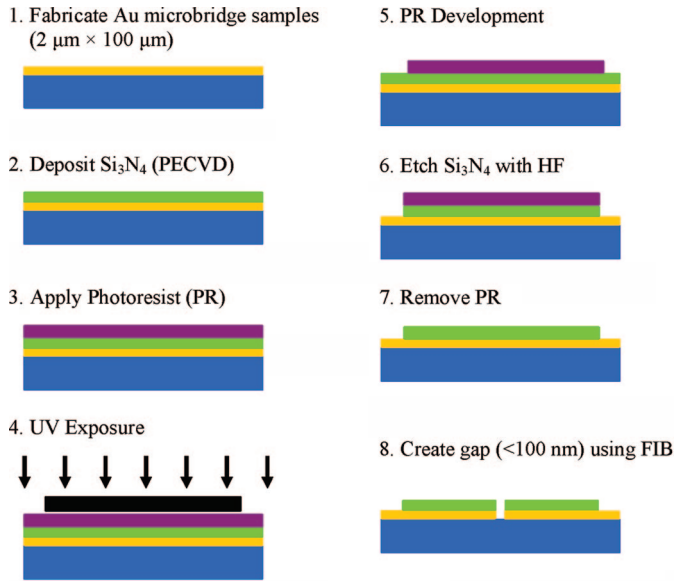

Figure 2. Procedure for the fabrication of Au nanogap samples for ASJ formation. Steps 2−6 delineate the openings for macroscale contact pads in the Si_3N_4 protecting layer. Steps 7 and 8 develop the nanometer-scale gap in the Au microbridge. Details of photolithography and lift-off processes for the fabrication of Au microbridge samples (step 1) are omitted for brevity.

RESULTS AND DISCUSSION

In order to determine appropriate potentials for electrochemical deposition and dissolution, cyclic voltammetric (CV) characterizations of gold in the electroplating media were always investigated first. In the iodide-containing electroplating medium (see Experimental Section for details of preparation), gold is present as AuI_2^- and AuI_4^-.[30] Figure 1 shows a typical cyclic voltammogram of a macroscale gold wire working electrode (WE) in this medium using another gold wire as both counter electrode (CE) and quasi-reference electrode (QRE). Comparisons were made among control experiments performed in blank solutions composed of (a) 50 mM $HClO_4$, (b) 50 mM $HClO_4$ containing 5 mM KI, and (c) 0.1 M KI (data not shown here) as well as literature results.[31] The redox peaks around 0 V correspond to a mixture of two processes:

$$Au + 2I^- \rightleftharpoons AuI_2^- + e^- \quad (2)$$

and

$$3I^- \rightleftharpoons I_3^- + 2e^- \quad (3)$$

while processes above 0.75 V may include the dissolution of Au into Au(III) as well as the oxidation of tri-iodide:

$$Au + 4I^- \rightarrow AuI_4^- + 3e^- \quad (4)$$

$$2I_3^- \rightarrow 3I_2 + 2e^- \quad (5)$$

and/or

$$3Au + 4I_3^- \rightarrow 3AuI_4^- + e^- \quad (6)$$

In light of these results for bare Au wire electrodes, fixed potential values in the region of $-300\ mV < E_{DC} < 300\ mV$ were selected for electrochemical deposition or dissolution of gold toward fabrication of ASJs in this electroplating medium.

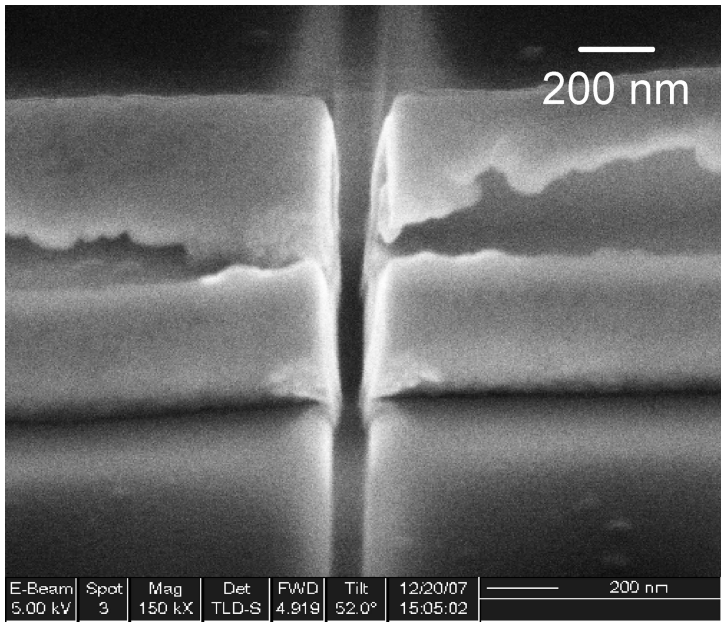

Figure 3. Plan view (52° tilt) SEM image of a typical sample after FIB milling.

For the ASJ electrochemical fabrication experiments, the WEs are Si_3N_4 (or SiO_2)-covered gold nanogap samples. These nanogaps were fabricated by focused ion beam milling of photolithographically fabricated, Si_3N_4-protected micrometer-scale Au bridges (see Figure 2 and Experimental Section for details). The typical gap width is ≤100 nm, as indicated in the SEM image in Figure 3. As in the CV experiments, a gold wire served as both CE and RE. Figure 4 shows a schematic diagram of the experiment. The impedance of the sample was monitored *in situ* by AC excitation. It should be noted that the WE here (the vertical sides of the Au nanogap) is actually a nanoelectrode, and its surface area is much smaller than that of the CE/RE (a macroscopic Au wire). Therefore, the same Au wire can be used as both the CE and the RE without significant drift in the RE potential. Since initially all samples were prepared as nanogaps, a negative value of E_{DC} was applied in order to grow gold in the gap. The nanogap can be closed by electrodeposition, even if the WE is isolated from the E_{DC} loop, for example, by disconnecting the WE from the potentiostat without actually terminating E_{DC}. However, the reaction rate is much slower, which is the desired result for a highly controllable process. Furthermore, if the applied bias, E_{DC}, and therefore the overpotential, is kept small, extremely slow reaction rates can be achieved, which allows the electrodeposition of ASJs to be manually terminated at a desired G value. This may be accomplished either by disconnecting the CE or by completely terminating E_{DC}.

Using this protocol, the fabrication can be controlled with a high degree of precision over the final conductance, and steps in the conductance during fabrication can be clearly observed. Typically, starting from a freshly prepared nanogap, the applied bias is initially set to a relatively large negative value, such as −250 mV, for a period of time determined by the initial width of the gap in order to narrow the gap through electrodeposition of Au. Subsequently, E_{DC} is decreased to a much smaller (*i.e.*, less negative) value to slow down the deposition, therefore allowing the deposition to be terminated at the desired G value. Normally, a Au ASJ can be formed in just a few minutes starting from an FIB-milled nanogap.

Shown in Figure 5 is a conductance−time trace acquired under small negative bias, $E_{DC} = -20$ mV, without connecting the WE (Au sample) to the potentiostat. As is evident from the figure, when the CE is immersed in the plating solution, thereby beginning the application of E_{DC} at $t = 50$ s, the conductance starts to increase. The current briefly (~20s) plateaus at $G \sim 1G_0$ at $t \sim 190$ s, indicating formation of an atomic-dimension Au junction. The conductance continues to increase until $t \sim 300$ s, when the CE is removed from the solution. The conductance of the sample thereafter remains constant near a value of $3G_0$, exhibiting small-scale fluctuations around the mean value $3G_0$ for as long as data were collected.

Utilizing this protocol, overdeposition may occur, especially when E_{DC} is too large. In this case, a positive small bias can be used to back-thin the nanowire *via* gold dissolution, thereby narrowing the junction. Just as for electrodeposition, electrodissolution can be performed in the "open-WE" mode, as indicated in Figure 6. Inset A shows that the conductance of the overgrown

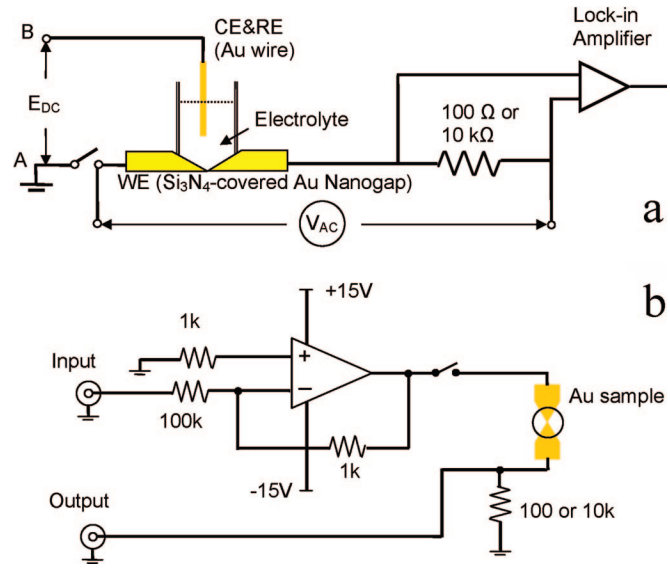

Figure 4. (a) Experimental configuration for electrochemical fabrication of atom-scale junctions. E_{DC} is set by the potentiostat and is equal to E(A) − E(B). (b) Electronic schematic for *in situ* monitoring of conductance variations during ASJ formation.

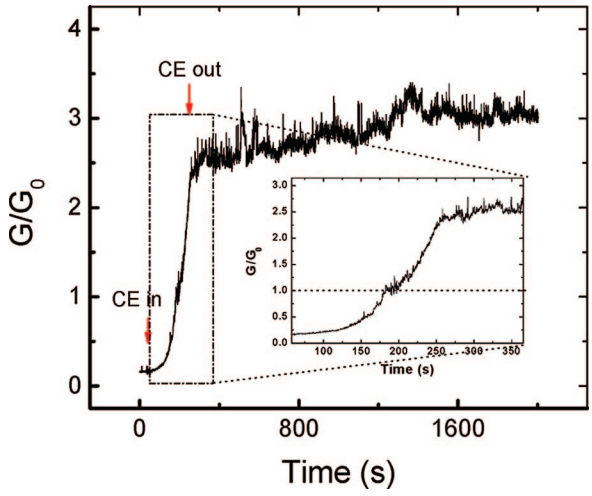

Figure 5. Conductance *versus* time trace during the formation of a gold atom-scale junction in the iodide-containing medium under a small negative bias (E_{DC} = −20 mV). The red arrows indicate the times at which the CE was put into or pulled out of the electrolyte. The WE (Au nanogap sample) was disconnected from the potentiostat throughout the deposition. (Inset) Expanded time trace of the steeply rising part of the conductance data.

junction decreases in stepwise fashion when the CE is immersed in the solution under the small positive bias of E_{DC} = 30 mV. When the conductance reached $1G_0$, the CE was removed from the solution, after which the conductance was stable at $\sim 1G_0$ for an extended period (inset B). Experiments with multiple samples under these conditions showed lifetimes up to 1 h. However, a small, slow increase or decrease in G was typically observed after removal of the CE, likely resulting from configuration variation or structural relaxation of the ASJ due to surface diffusion of gold atoms at room temperature.

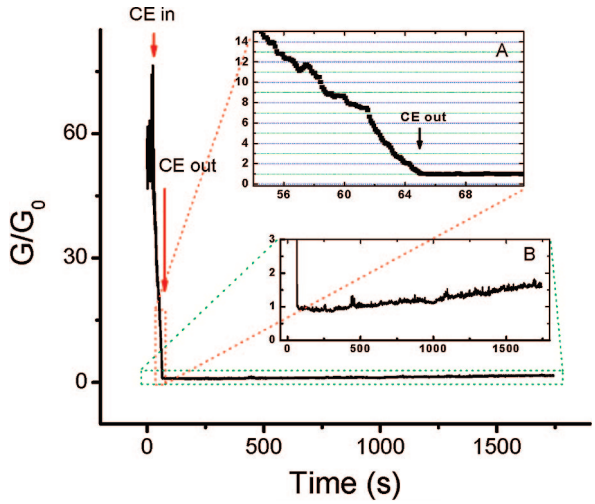

Figure 6. Conductance *versus* time trace during the dissolution of an overdeposited gold junction in the iodide medium under a small positive bias, E_{DC} = 30 mV. The arrows indicate the times at which the CE was put into or pulled out of the electrolyte. The WE (Au nanowire sample) was disconnected from the potentiostat throughout the experiment. (Inset A) Expanded time trace of the conductance just prior to terminating dissolution. (Inset B) Expanded time trace of the junction showing its stability over ~30 min at 300 K.

The conductance−time traces discussed above indicate that, if a sufficiently small E_{DC} value is used in open-WE mode, the electrodissolution or electrodeposition reactions are slowed significantly. It can take tens of seconds or even longer for the conductance to change by $1G_0$. The controllability of fabrication of ASJs is greatly enhanced under these conditions because the CE may be removed at any desired conductance value. Furthermore, the slow and controllable kinetics under these conditions suggest that this mode of operation can be employed to fabricate other nanostructures, such as atom-size nanogaps with desired gap spacings.

It is interesting to note that not every conductance−time trace shows conductance plateaus, especially in the initial few cycles. Typically, multiple deposition and dissolution cycles increase the propensity for a given junction to manifest stepwise conductance changes concomitant with higher stability nanojunctions. A similar phenomenon has also been reported both in ultrahigh vacuum[32] and in electrolyte.[24,28,29] This behavior was attributed to improved crystallinity of the structures formed and was termed "electrochemical annealing" by Tao *et al.*[24] Thus, the lack of conductance steps in the initial conductance−time traces may arise from slow structural relaxation between configurations in the initial deposition and dissolution steps.

Mechanically robust ASJs are obtained in the iodide-containing medium after several deposition/dissolution cycles. Their lifetimes typically range from tens of minutes to hours, easily long enough for further studies of the properties of the ASJs and for chemical sensing applications. To test their robustness, these ASJs

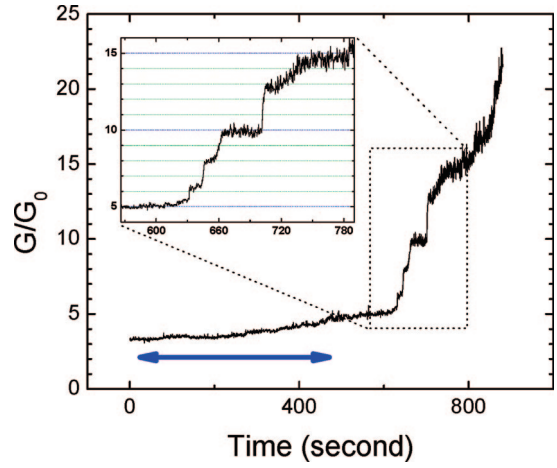

Figure 7. Conductance *versus* time trace of a gold ASJ under conditions of mechanical disturbance (see text for details). The thick blue line with arrows marks the time course of the mechanical disturbance. (Inset) Expanded time trace of the ASJ rearrangement to larger conductance values subsequent to the disturbance.

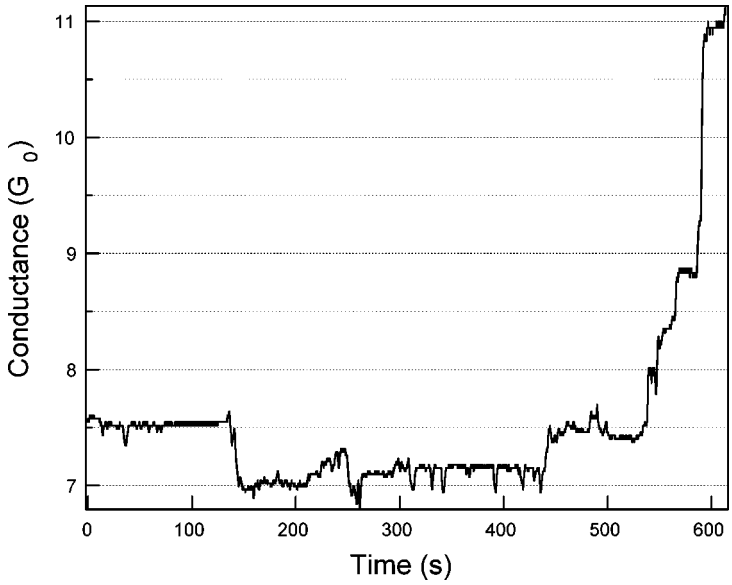

Figure 8. Stability of an ASJ fabricated in 2 mM $HAuCl_4$/50 mM $HClO_4$ containing ~0.1 mM L-cysteine as additive.

were subjected to a mechanical disturbance, as shown in Figure 7. The ASJ conductance was monitored *in situ* when a small syringe was used to first remove electrolyte from the PDMS cell, then rinse the sample surface by adding and removing two aliquots (~50 μL) of DI water in the well. The ASJ was stable during the course of the rinsing/filling steps but became unstable afterward, eventually spontaneously overgrowing the small-scale dimensions ($G < 20G_0$) most useful for sensing experiments. The inset shows the evident stepwise increase of conductance during the overgrowth of the ASJ.

Although the special open-WE operation mode enhances the controllability of fabrication, the electrolyte also plays an important role in determining controllability and stability of ASJs. When ASJs were fabricated in $HClO_4$ electrolyte (50 mM $HClO_4$ containing 2 mM $HAuCl_4$) using open-WE mode, the yield was much lower, and the lifetimes of ASJs obtained were always much shorter (<100 s, data not shown). However, if a small amount of cysteine (enough to yield ~0.1−0.2 mM) is added as an organic modifier, the ASJ yield increases dramatically, and the lifetimes of the junctions are improved, as shown in Figure 8, although still not as long as those fabricated in the iodide medium.

ASJ stability and lifetime are correlated with the surface morphology of the Au deposit. Shown in Figure 9 are SEM images of the Au deposit formed in the three electroplating media examined. As is evident from these images, electrodeposition in unmodified $HClO_4$ produces coarse grains and roughened surface morphology, while the cysteine-containing medium yields much denser and smoother deposits. The deposit formed in the iodide medium is even finer-grained and more compact, which correlates with this medium being more favorable for the fabrication of stable ASJs.

It has been reported that both iodide ions and cysteine strongly influence the size and crystallographic orientation of electrodeposited gold nanoparticles,[33] and the importance of smooth and compact surface morphology for the stability of the nanostructures has also been discussed by other researchers.[26,34,35] The reason that different media produce deposits of dramatically different surface morphology is likely related to molecular (or ionic) adsorption. Cysteine, for example, contains a thiol group, which is well-known to bind to gold surfaces *via* specific Au−S bonding. Iodide also bonds to Au *via* strong, specific ionic adsorption. The strong adsorption of these species can significantly hinder heterogeneous electron transfer,[36] thereby affecting the kinetics of electrodeposition and the growth of metal deposits. So it is likely that adsorption of electrolyte constituents is the major contributor to the stabilization of ASJs, a conclusion consistent with other deposition studies, as well.[37–39] For example, Kiguchi *et al.* found adsorption of either anions (SO_4^{2-}) or molecular hydrogen could stabilize monatomic gold wires.[37] Tao *et al.* studied the correlation between the binding strength of three different molecules and the degree of adsorbate effects on the lifetime of atomically thin gold nanowires and found that strong binding of the adsorbate molecules to the surface of the nanowires can significantly lower the surface energy, thus prolonging the lifetime of the nanowire at a given atomic configuration.[38]

Finally, we turn our attention to the surprising result that the electrochemical process proceeds, even if the WE is open or not in direct contact with the CE. Note that E_{DC}, as set by the potentiostat, is defined as the WE potential with respect to the RE, which is the same as the CE in this two-electrode system (*i.e.*, $E_{DC} = E_{WE} - E_{CE}$). In the regular operation mode of three-electrode potentiostatically controlled electrochemical experiments, the WE is always connected to the earth ground of the potentiostat. Therefore, a negative value of E_{DC} means a positive voltage applied on the CE with respect to the earth ground. When the WE is disconnected, its potential is located somewhere between the potential of the CE, E_{CE}, and earth ground, E_{ground}. This small and "unknown" potential difference between WE and CE perturbs the electrochemical equilibrium on the WE (as well as the CE) surface toward a new equilibrium position. As configured in the present experiments, this leads to slow deposition or dissolution processes involving the electrode surface. Furthermore, the lack of di-

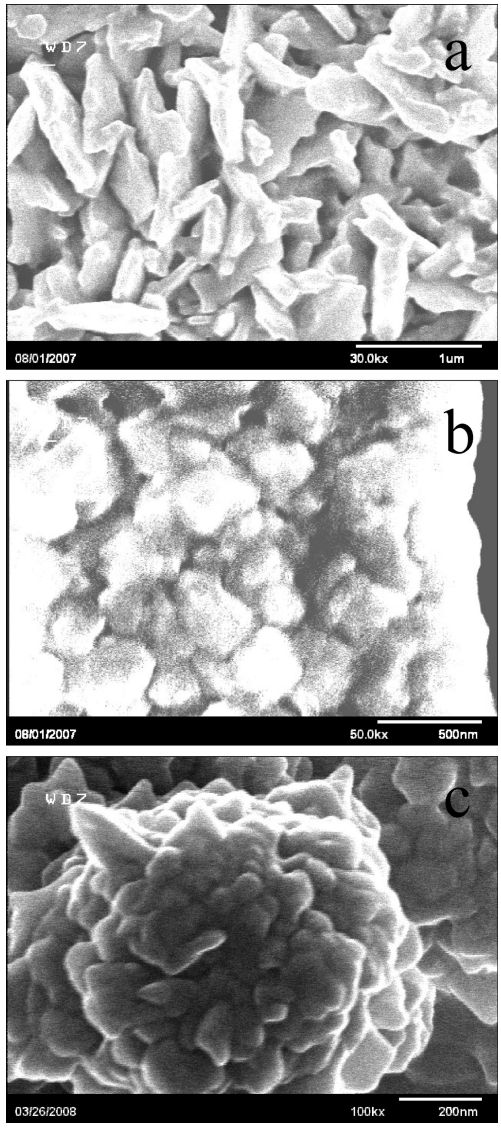

Figure 9. SEM images of gold deposited in (a) 2 mM $HAuCl_4$ in 50 mM $HClO_4$; (b) 2 mM $HAuCl_4$ in 50 mM $HClO_4$ containing ~0.2 mM cysteine; (c) the iodide medium. Note the scale bars are 1 μm (a), 500 nm (b), and 200 nm (c). Gold deposits shown were obtained on macroscale wires in the same media used to fabricate ASJs.

rect electrical contact between WE and CE through a controlled electrical circuit prevents continuous current flow though the system. In this open-WE mode of operation, no DC current is measured in the WE/CE circuit. Because this current arises from electrochemical changes involving a few Au atoms at a time, it is too small to be measurable. Instead, the AC current across the WE is measured because it amplifies the significant conductance change upon conversion of the gap to an atom-scale junction. The two-electrode system is especially vulnerable to uncompensated *iR* drops, and small swings in applied potential can accelerate the heterogeneous electron transfer processes responsible for junction formation. Thus, the electrochemical equilibrium is exceptionally sensitive to the exact conditions under which electron transfer occurs, such that small changes in E_{DC} can have dramatic effects on rates of electron transfer, rendering the fabrication difficult to control. For these reasons, the open-WE protocol described here, although unconventional, has a number of attractive features within the special context of creating ASJs.

CONCLUSIONS

A novel mode of electrochemical nanofabrication employing an open working electrode has been developed for the highly controllable formation of atom-scale junctions. Extremely slow electrodeposition and electrodissolution rates can be achieved by using this unique open-WE mode, making it possible to attain control over the placement of the last few atoms. This heightened level of control over electron transfer rates makes it possible to realize high yields of atom-scale junctions with enhanced mechanical stability. Gold ASJs can be fabricated at any conductance value because it is possible to monitor the conductance and halt the electrochemical process at the desired end point. In addition, this open-WE mode can be used to prepare Si_3N_4- or SiO_2-protected Au nanogaps by carefully closing nanogaps ($d \sim 100$ nm) prepared in a 1−2 μm wide Au microbridge by FIB milling. The stability as well as the yield of ASJs depends sensitively on the nature of the electroplating medium, as evidenced by the strong correlation between ASJ stability and surface morphology of the deposit, both being related to molecular or ionic adsorption. Gold ASJs fabricated in iodide-containing media can be stable for periods up to hours, demonstrating their promise for chemical sensing applications.

EXPERIMENTAL SECTION

Sample Preparation. Figure 2 shows the sample fabrication procedure schematically. Bowtie-shaped Au films (3 nm Cr/30 nm Au), containing a 2 μm wide × 100 μm long microbridge in the center of each "bowtie" were deposited on Si wafers covered by a 500 nm thermal oxide (Silicon Quest International, Santa Clara, CA) using standard photolithography and lift-off techniques (step 1). Afterward, a thin layer of dielectric material Si_3N_4 (or SiO_2, typically 100 nm thick) was deposited over the entire sample surface by plasma-enhanced chemical vapor deposition (step 2). After another photolithography step to expose the contact pads at both ends of each sample for external electrical contact (steps 3−6), a thin nanoslit (<100 nm in width) was milled through both the Si_3N_4 layer as well as the underlying Au (steps 7 and 8) by an FEI Strata DB235 dual-source focused ion beam (FIB). The nanoslit was oriented perpendicular to the long axis of the microbridge, thereby breaking the bridge so that the nanocontact could form in the nanogap electrochemically. Figure 3 shows an SEM image of a nanogap sample after FIB milling. Protecting the Au surface by the insulating layer is essential because it both reduces solution-phase ionic contributions to the current and focuses the Au deposition to the small area between

Au pads in the nanoslit. After FIB milling, the samples were immersed in concentrated HNO_3 for 25 min followed by rinsing with deionized (DI) water to remove residual solvent-accessible Ga^+ ion deposited during FIB milling. After cleaning, the samples were stored under dry N_2 to avoid contamination prior to the electrochemical experiments.

Electroplating Solution Preparation. Three kinds of non-cyanide media were explored: (1) 2.0 mM $HAuCl_4$ (Aldrich, 99.999%) in 50 mM $HClO_4$ (Sigma-Aldrich, 70%, distilled 99.999%), (2) 2.0 mM $HAuCl_4$ in 50 mM $HClO_4$ containing 0.1−0.2 mM L-cysteine (Sigma, >99%), and (3) an iodide-containing medium similar to that reported by Umeno *et al.*[30] In detail to prepare solution (3), a piece of 0.25 mm (diameter) gold wire (99.95%, Alfa Aesar) was cleaned in freshly prepared piranha solution (7:3 H_2SO_4/H_2O_2) for 20−30 min. After rinsing with DI water, it was dissolved in an aqueous solution of 3% (w/v) I_2 (Sigma-Aldrich, 99.8%, ACS Reagent) and 2% (w/v) KI (Fisher, Certified ACS) by shaking for >2 h until the solution became saturated. L-(+)-Ascorbic acid (Sigma) was then added to the solution until its color turned from dark brown to transparent, indicating that the excess I_2 was reduced to I^- by the ascorbic acid.

Electrochemical Experiments and Fabrication. Cyclic voltammetry (CV) experiments were carried out with a commercial potentiostat (Pine Instruments, model AFCBP1) using a piece of 0.25 mm (diameter) gold wire (Alfa Aesar, 99.95%) as the working electrode (WE) and another piece of gold wire (same diameter) as both counter (CE) and quasi-reference electrode (QRE) in all three electroplating media described above. Prior to electrochemical experiments, the gold wires were carefully cleaned in freshly prepared piranha solution. In the electrochemical fabrication process, a DC potential, E_{DC}, was applied by the potentiostat between the counter electrode (a 0.25 mm Au wire, that also served as QRE) and the earth ground of the potentiostat, which in most cases was not connected to the gold nanogap sample (the WE). Thus, the WE was isolated from the E_{DC} loop, and its potential was different than the CE potential. Depending on the value of E_{DC}, the electrochemical process proceeding on the sample gold surface could be either electrodeposition or electrodissolution. The impedance across the nanogap was monitored *in situ* by measuring the AC voltage drop across a series resistance (10 kΩ or 100 Ω) under a small AC excitation, V_{AC}, using a lock-in amplifier (Stanford Research Systems model SR830). A schematic diagram of experimental apparatus is shown in Figure 4a. Several constraints were placed on the experimental parameters by the special nature of the ASJs and the unique electrochemical process. First, the frequency of AC excitation was limited to a small value (<10 Hz) to minimize parasitic capacitance. Second, the amplitude of V_{AC} was kept as small as possible (typically 100 μV) to minimize the disturbance of the electrochemical equilibrium at the electrode/solution interface. In order to further decrease V_{AC}, a simple circuit (Figure 4b) was designed that allows the input AC excitation from the lock-in amplifier to be decreased by a factor of 100. In experiments, the amplitude of AC excitation was usually set at 10 mV; therefore, the actual V_{AC} applied across the sample and the series resistor was 100 μV. For all the electrochemical fabrication experiments, the electrolyte was held in a PDMS well (~3 mm deep × 7 mm diameter) mounted directly over the nanoslit.

Acknowledgment. This work was supported by the National Science Foundation through Grant CHE 08-07816 and by the U.S. Army Corps of Engineers (W9132T-07-2-003). The authors gratefully acknowledge the technical assistance of G. Qian in the early stages of this project, and the advice of Patrick Fay on microfabrication.

REFERENCES AND NOTES

1. Ferry, D. K. Nanowires in Nanoelectronics. *Science* **2008**, *319*, 579–580.
2. Melosh, N. A.; Boukai, A.; Diana, F.; Gerardot, B.; Badolato, A.; Petroff, P. M.; Heath, J. R. Ultrahigh-Density Nanowire Lattices and Circuits. *Science* **2003**, *300*, 112–115.
3. Favier, F.; Walter, E. C.; Zach, M. P.; Benter, T.; Penner, R. M. Hydrogen Sensors and Switches from Electrodeposited Palladium Mesowire Arrays. *Science* **2001**, *293*, 2227–2231.
4. Walter, E. C.; Penner, R. M.; Liu, H.; Ng, K. H.; Zach, M. P.; Favier, F. Sensors from Electrodeposited Metal Nanowires. *Surf. Interface Anal.* **2002**, *34*, 409–412.
5. Im, Y.; Lee, C.; Vasquez, R. P.; Bangar, M. A.; Myung, N. V.; Menke, E. J.; Penner, R. M.; Yun, M. H. Investigation of a Single Pd Nanowire for Use as a Hydrogen Sensor. *Small* **2006**, *2*, 356–358.
6. Liu, Z.; Searson, P. C. Single Nanoporous Gold Nanowire Sensors. *J. Phys. Chem. B* **2006**, *110*, 4318–4322.
7. Wanekaya, A. K.; Chen, W.; Myung, N. V.; Mulchandani, A. Nanowire-Based Electrochemical Biosensors. *Electroanal.* **2006**, *18*, 533–550.
8. Li, C. Z.; He, H. X.; Bogozi, A.; Bunch, J. S.; Tao, N. J. Molecular Detection Based on Conductance Quantization of Nanowires. *Appl. Phys. Lett.* **2000**, *76*, 1333–1335.
9. Lin, H. Y.; Chen, H. A.; Lin, H. N. Fabrication of a Single Metal Nanowire Connected with Dissimilar Metal Electrodes and its Application to Chemical Sensing. *Anal. Chem.* **2008**, *80*, 1937–1941.
10. Sudeep, P. K.; Joseph, S. T. S.; Thomas, K. G. Selective Detection of Cysteine and Glutathione using Gold Nanorods. *J. Am. Chem. Soc.* **2005**, *127*, 6516–6517.
11. Li, C. Z.; Sha, H.; Tao, N. J. Adsorbate Effect on Conductance Quantization in Metallic Nanowires. *Phys. Rev. B* **1998**, *58*, 6775–6778.
12. Bogozi, A.; Lam, O.; He, H. X.; Li, C. Z.; Tao, N. J.; Nagahara, L. A.; Amlani, I.; Tsui, R. Molecular Adsorption onto Metallic Quantum Wires. *J. Am. Chem. Soc.* **2001**, *123*, 4585–4590.
13. Xu, B. Q.; He, H. X.; Boussaad, S.; Tao, N. J. Electrochemical Properties of Atomic-Scale Metal Wires. *Electrochim. Acta* **2003**, *48*, 3085–3091.
14. Kiguchi, M.; Djukic, D.; van Ruitenbeek, J. M. The Effect of Bonding of a CO Molecule on the Conductance of Atomic Metal Wires. *Nanotechnology* **2007**, *18*, 035205/1–035205/5.
15. Castle, P. J.; Bohn, P. W. Interfacial Scattering at Electrochemically Fabricated Atom-Scale Junctions between Thin Gold Film Electrodes in a Microfluidic Channel. *Anal. Chem.* **2005**, *77*, 243–249.
16. Zhang, Y. M.; Terrill, R. H.; Bohn, P. W. Chemisorption and Chemical Reaction Effects on the Resistivity of Ultrathin Gold Films at the Liquid−Solid Interface. *Anal. Chem.* **1999**, *71*, 119–125.
17. Landauer, R. Spatial Variation of Currents and Fields Due to Localized Scatterers in Metallic Conduction. *IBM J. Res. Dev.* **1957**, *1*, 223–231.
18. Buttiker, M.; Imry, Y.; Landauer, R.; Pinhas, S. Generalized Many-Channel Conductance Formula with Application to Small Rings. *Phys. Rev. B* **1985**, *31*, 6207–6215.
19. Ohnishi, H.; Kondo, Y.; Takayanagi, K. Quantized Conductance through Individual Rows of Suspended Gold Atoms. *Nature* **1998**, *395*, 780–783.
20. Agrait, N.; Yeyati, A. L.; van Ruitenbeek, J. M. Quantum Properties of Atomic-Sized Conductors. *Phys. Rep.* **2003**, *377*, 81–279.
21. van Ruitenbeek, J. M.; Alvarez, A.; Pineyro, I.; Grahmann, C.; Joyez, P.; Devoret, M. H.; Esteve, D.; Urbina, C. Adjustable Nanofabricated Atomic Size Contacts. *Rev. Sci. Instrum.* **1996**, *67*, 108–111.
22. Yanson, A. I.; Bollinger, G. R.; van den Brom, H. E.; Agrait, N.; van Ruitenbeek, J. M. Formation and Manipulation of a Metallic Wire of Single Gold Atoms. *Nature* **1998**, *395*, 783–785.
23. He, H. X.; Boussaad, S.; Xu, B. Q.; Li, C. Z.; Tao, N. J. Electrochemical Fabrication of Atomically Thin Metallic Wires and Electrodes Separated with Molecular-Scale Gaps. *J. Electroanal. Chem.* **2002**, *522*, 167–172.
24. Li, C. Z.; Bogozi, A.; Huang, W.; Tao, N. J. Fabrication of Stable Metallic Nanowires with Quantized Conductance. *Nanotechnology* **1999**, *10*, 221–223.
25. Xiang, J.; Liu, B.; Wu, S. T.; Ren, B.; Yang, F. Z.; Mao, B. W.; Chow, Y. L.; Tian, Z. Q. A Controllable Electrochemical Fabrication of Metallic Electrodes with a Nanometer/

Angstrom-Sized Gap Using an Electric Double Layer as Feedback. *Angew. Chem., Int. Ed.* **2005**, *44*, 1265–1268.
26. Liu, B.; Xiang, J.; Tian, J. H.; Zhong, C.; Mao, B. W.; Yang, F. Z.; Chen, Z. B.; Wu, S. T.; Tian, Z. Q. Controllable Nanogap Fabrication on Microchip by Chronopotentiometry. *Electrochim. Acta* **2005**, *50*, 3041–3047.
27. Li, C. Z.; Tao, N. J. Quantum Transport in Metallic Nanowires Fabricated by Electrochemical Deposition/Dissolution. *Appl. Phys. Lett.* **1998**, *72*, 894–896.
28. Li, J. Z.; Yamada, Y.; Murakoshi, K.; Nakato, Y. Sustainable Metal Nano-contacts Showing Quantized Conductance Prepared at a Gap of Thin Metal Wires in Solution. *Chem. Commun.* **2001**, 2170–2171.
29. Meszaros, G.; Kronholz, S.; Karthauser, S.; Mayer, D.; Wandlowski, T. Electrochemical Fabrication and Characterization of Nanocontacts and nm-Sized Gaps. *Appl. Phys. A: Mater. Sci. Process.* **2007**, *87*, 569–575.
30. Umeno, A.; Hirakawa, K. Fabrication of Atomic-scale Gold Junctions by Electrochemical Plating using a Common Medical Liquid. *Appl. Phys. Lett.* **2005**, *86*, 054103.
31. Qi, P. H.; Hiskey, J. B. Electrochemical-Behavior of Gold in Iodide Solutions. *Hydrometallurgy* **1993**, *32*, 161–179.
32. Rubio, G.; Agrait, N.; Vieira, S. Atomic-Sized Metallic Contacts: Mechanical Properties and Electronic Transport. *Phys. Rev. Lett.* **1996**, *76*, 2302–2305.
33. El-Deab, M. S.; Sotomura, T.; Ohsaka, T. Size and Crystallographic Orientation Controls of Gold Nanoparticles Electrodeposited on GC Electrodes. *J. Electrochem. Soc.* **2005**, *152*, C1–C6.
34. Kervennic, Y. V.; Van der Zant, H. S. J.; Morpurgo, A. F.; Gurevich, L.; Kouwenhoven, L. P. Nanometer-Spaced Electrodes with Calibrated Separation. *Appl. Phys. Lett.* **2002**, *80*, 321–323.
35. Kiguchi, M.; Miura, S.; Murakoshi, K. Fabrication of Stable Metal Nanowire Showing Conductance Quantization in Solution. *Surf. Sci.* **2007**, *601*, 4127–4130.
36. Porter, M. D.; Bright, T. B.; Allara, D. L.; Chidsey, C. E. D. Spontaneously Organized Molecular Assemblies. 4. Structural Characterization of Normal-Alkyl Thiol Monolayers on Gold by Optical Ellipsometry, Infrared-Spectroscopy, and Electrochemistry. *J. Am. Chem. Soc.* **1987**, *109*, 3559–3568.
37. Kiguchi, M.; Konishi, T.; Murakoshi, K. Conductance Bistability of Gold Nanowires at Room Temperature. *Phys. Rev. B* **2006**, *73*, 125406-1–125406-5.
38. He, H. X.; Shu, C.; Li, C. Z.; Tao, N. J. Adsorbate Effect on the Mechanical Stability of Atomically Thin Metallic Wires. *J. Electroanal. Chem.* **2002**, *522*, 26–32.
39. Kiguchi, M.; Konishi, T.; Miura, S.; Murakoshi, K. Mechanical Fabrication of Metal Nano-Contacts Showing Conductance Quantization under Electrochemical Potential Control. *Physica E* **2005**, *29*, 530–533.